Near-Infrared Light-Mediated Antimicrobial Based on $Ag/Ti_3C_2T_x$ for Effective Synergetic Antibacterial Application

Xiaoquan Zhu, ‡[a] Yingnan Zhu, ‡[b] Jia Ke,[b] Bahreselam Sielu Abraha,[a] Yang Li,[a] Wenchao Peng,[a] Fengbao Zhang,[a] Xiaobin Fan*[a] and Lei Zhang*[b]

[a] School of Chemical Engineering and Technology, State Key Laboratory of Chemical Engineering, Collaborative Innovation Center of Chemical Science and Engineering, Tianjin University, Tianjin 300072, People's Republic of China.

[b] School of Chemical Engineering and Technology, Frontier Science Center for Synthetic Biology and Key Laboratory of Systems Bioengineering (MOE), Tianjin University, Tianjin 300072, People's Republic of China.

‡These authors contributed equally to this work

*E-mail: xiaobinfan@tju.edu.cn; lei_zhang@tju.edu.cn

Table S1. Value of 2θ and β from the XRD pattern of $Ag/Ti_3C_2T_x$.

2θ (°)	cosθ	β(rad)	D (nm)	$\overline{D}$ (nm)
38.127	0.945	0.00651	23.621	22.810
44.307	0.926	0.00782	20.070	
64.475	0.846	0.00795	21.590	
77.390	0.780	0.00717	25.960	

Scherrer Equation: $D= k\bullet\lambda/(\beta\bullet\cos\theta)$. k=0.943, λ=0.154 nm

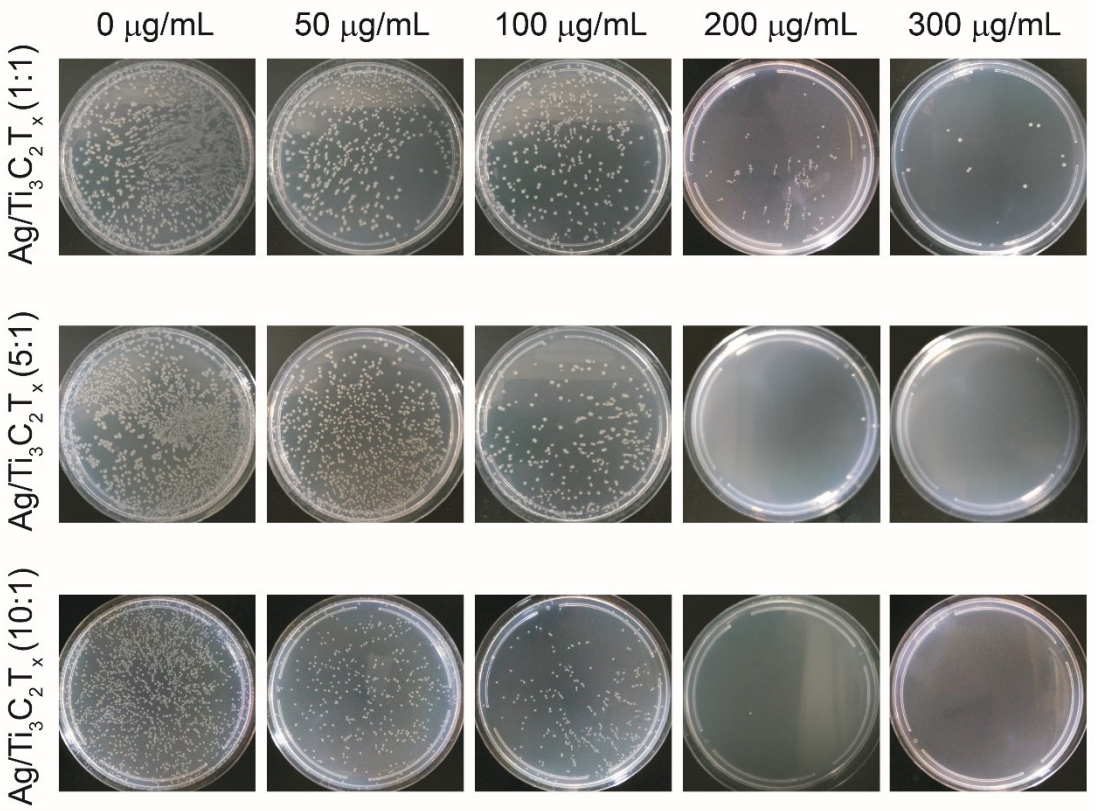

Figure S1. Photographs of bacterial colonies formed without NIR irradiation after incubation with different concentrations of $Ag/Ti_3C_2T_x$ (1:1), $Ag/Ti_3C_2T_x$ (5:1) and $Ag/Ti_3C_2T_x$ (10:1).

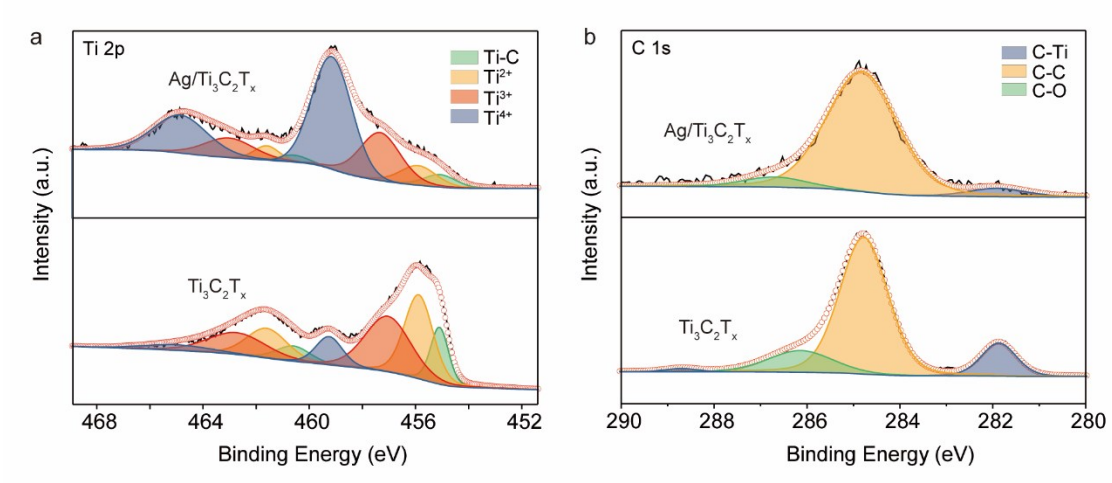

Figure S2. High-resolution XPS spectra of (a) Ti 2p and (b) C1s of $Ag/Ti_3C_2T_x$ composites and $Ti_3C_2T_x$.

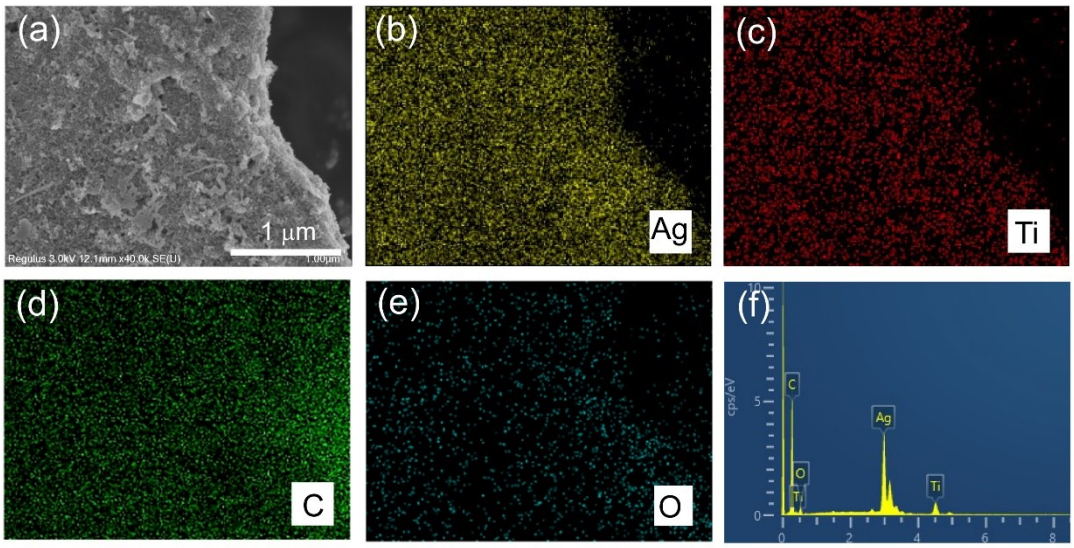

Figure S3. (a) the SEM image of $Ag/Ti_3C_2T_x$ composite, element mapping images for (b) Ag, (c) Ti and (d) C. (e) EDS spectrum of $Ag/Ti_3C_2T_x$ composite.

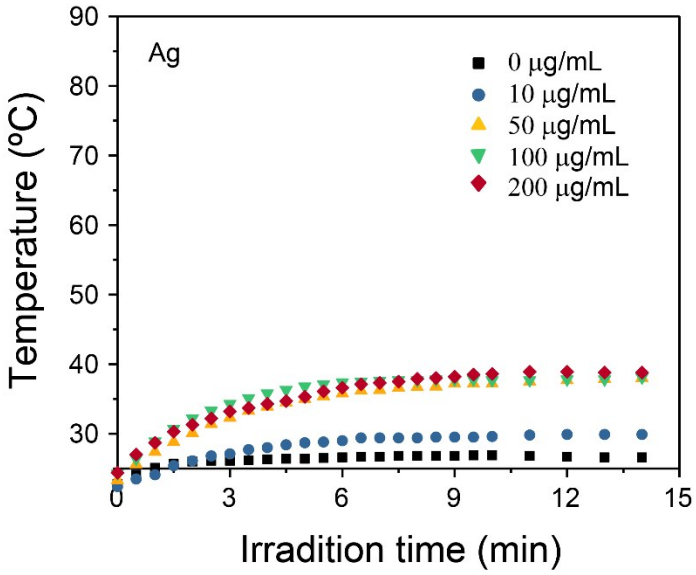

Figure S4. Temperature evolution curves of suspensions containing different concentrations of Ag NPs.

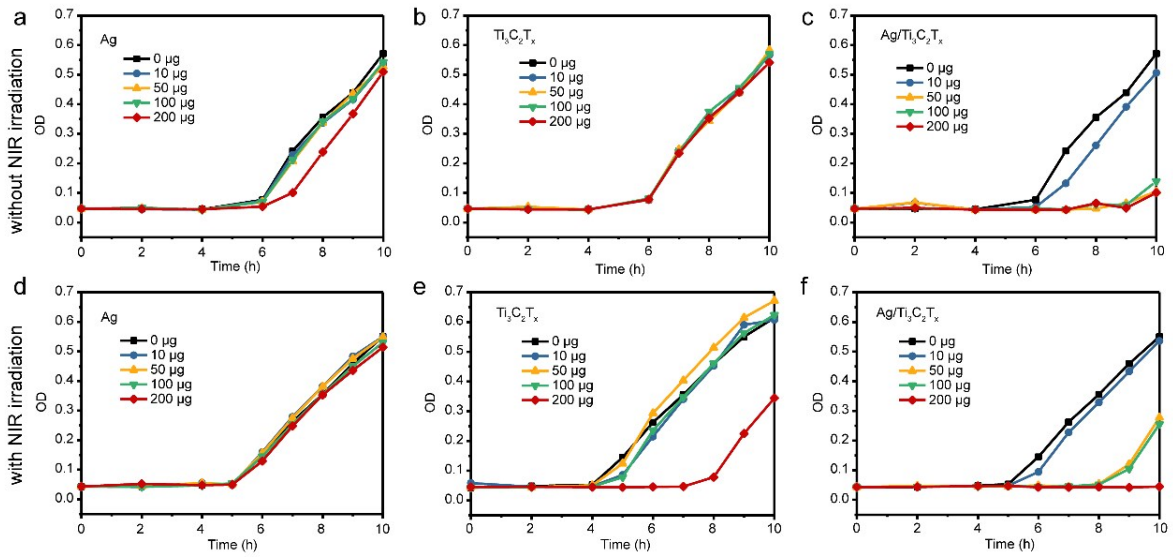

Figure S5. Bacterial growth curves of *S. aureus* after incubating with different concentrations of (a) Ag, (b) $Ti_3C_2T_x$ and (c) $Ag/Ti_3C_2T_x$ without NIR irradiation; and (d) Ag, (e) $Ti_3C_2T_x$ and (f) $Ag/Ti_3C_2T_x$ with NIR irradiation.

Table S2 Comparison of some nanomaterial with the photothermal effect for antibacterial

Antibacterial mechanism	NIR laser	Nanomaterial concentration	bacteria	Bacterial concentration	Antibacterial activity	Cell type	Cell viability	Ref.
PTT	808 nm, 0.75 W/cm^2, 10 min	0.1 mg/ml	S. aureus/ E. coli	2-3×10^8	~100%	NIH/3T3 cells	~90%	1
PTT	808 nm, 1.5 W/cm^2, 10min	0.8mg/ml	S. aureus/ E. coli	10^6-10^7	99%	CHO-K1 cells	87%	2
PTT	470 nm, 1 W/cm^2, 15min	0.1-0.2 mg/ml	S. aureus / E. coli	2×10^4	80-90%	mouse splenocytes	60-80%	3
PTT	808 nm, 1.0 W/cm^2, 10min	0.15 mg/ml	B. subtilis / E. coli	1.0 × 10^5	97% / 100%	HUVECs	~85%	4
PTT	808 nm, 2 W/cm^2, 10min	0.2 mg/ml	S. aureus/ E. coli	10^6–10^7	90%	HepG2 cells, BRL-3A and BV2 cells	~80%	5
PTT, Ag$^+$	808 nm, 1W/cm^2, 5min	0.25-0.5 mg/ml	S. aureus/ E. coli	2 × 10^5	>90%	L929 cells	20-80%	6
PTT, Ag$^+$	808 nm, 0.5 W/cm^2,	2 mg/ml	S. aureus/ E. coli	/	99%/97%	HUVECs	~10%	7
PTT, PDT	808 nm 2 W/cm^2, 3min	0.12-0.14 mg/ml	E. coli/ S. aureus	1 × 10^6	91.01% /97.57%	/	/	8
PTT, Ag$^+$	808 nm, 1.0 W/cm^2, 8 min	0.1 mg/ml	E. coli	/	~100%	MGC 803 cells	~80%	9
PTT, peroxidative catalyzation	808 nm, 1.0 W/cm^2, 10min	0.2 mg/ml	E. coli / S. aureus	10^5	96.8%/95.2%	NIH 3T3 cells	~80%	10
PTT, Ag$^+$	808 nm, 0.3 W/cm^2, 10min	15 μg/ml	E. coli	10^8	~100%	SW620 cells and MH-S cells	~75%	11
PTT, Ag$^+$	808 nm, 1.5 W/cm^2, 15 min	0.2 mg/ml	E. coli/ S. aureus	10^8	~100%	NIH 3T3 cells	>82%	This work

Nanomaterials	GO	GO	Graphene quantum dots	Nano-MoS_2	MoS_2	Au-Ag@SiO_2 NCs	MoO_3-x-Ag	Au@Bi_2S_3	PEG-Au@Ag	PDA@Au-HAp	RGO/Ag	Ag/$Ti_3C_2T_x$

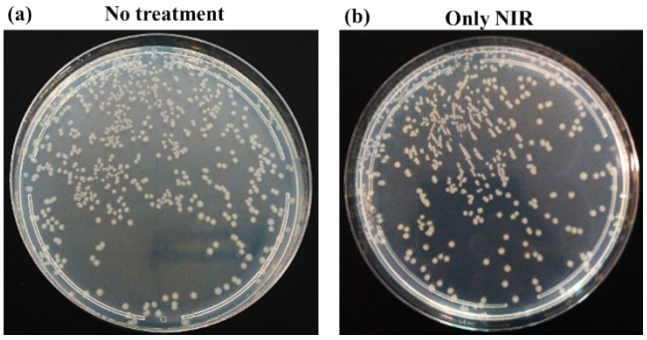

Figure S6. Photographs of *E.coli* bacterial colonies formed (a) without treatment, (b) with only NIR light irradiation.

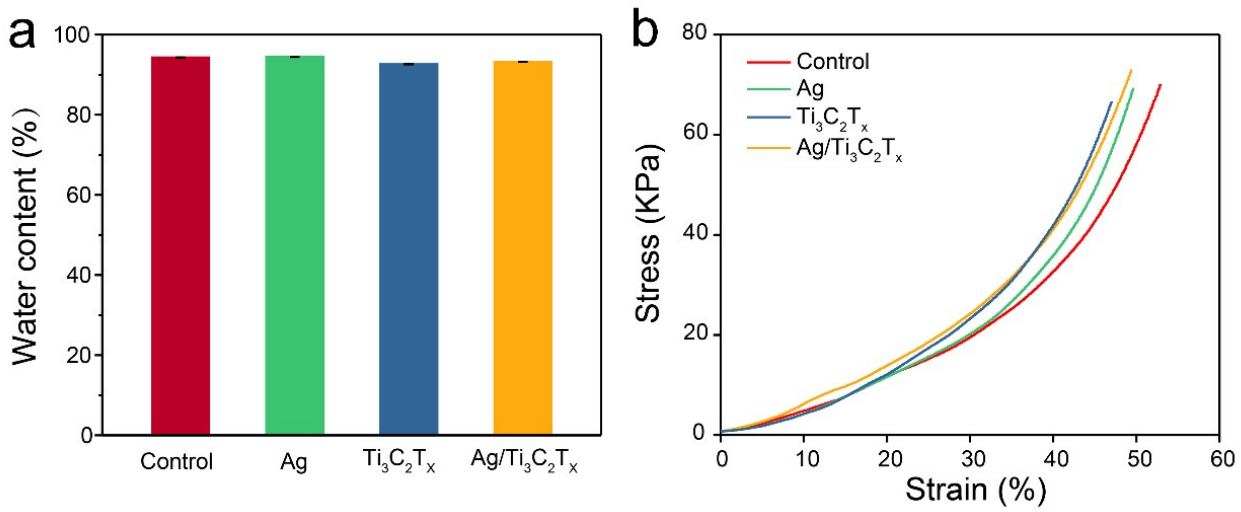

Figure S7. (a) The water content and (b) Compressive stress-strain curves of Ag, $Ti_3C_2T_x$ and Ag/$Ti_3C_2T_x$ embedded hydrogels

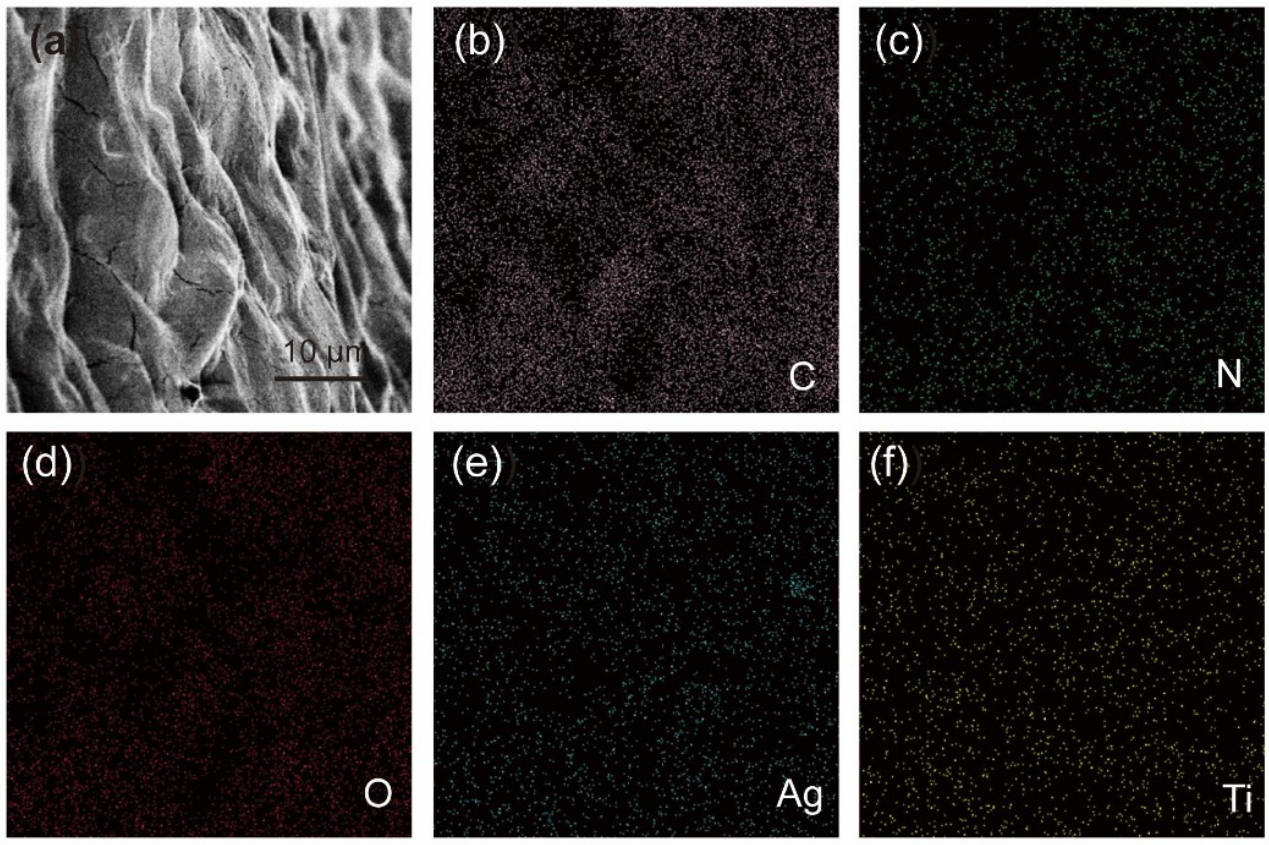

Figure S8. The SEM images of $Ag/Ti_3C_2T_x$ hydrogel and element mapping images for (b) C, (c) N, (d) O, (e) Ag and (f) Ti.

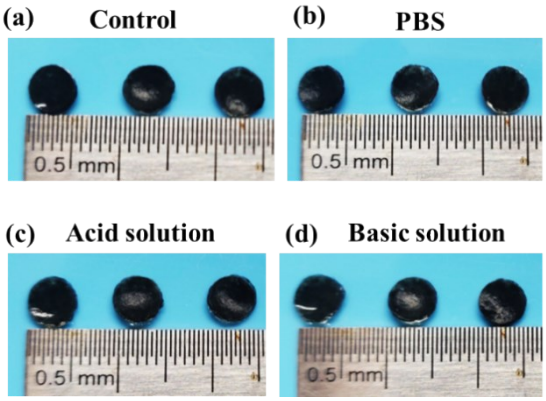

Figure S9. The morphology and size of $Ag/Ti_3C_2T_x$ hydrogel (a) before immersion and immersed in (b) PBS, (c) acid solution (pH=2.5) and (d)basic solution (pH=12).

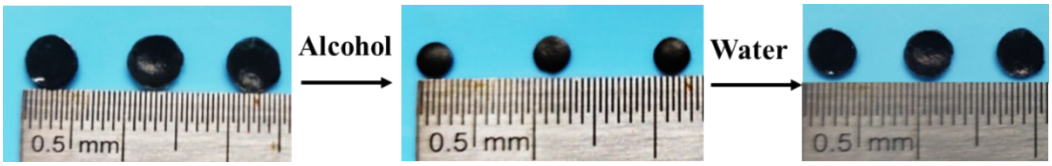

Figure S10. The morphology and size of $Ag/Ti_3C_2T_x$ hydrogel after dehydrated in alcohol and rehydrated in water.

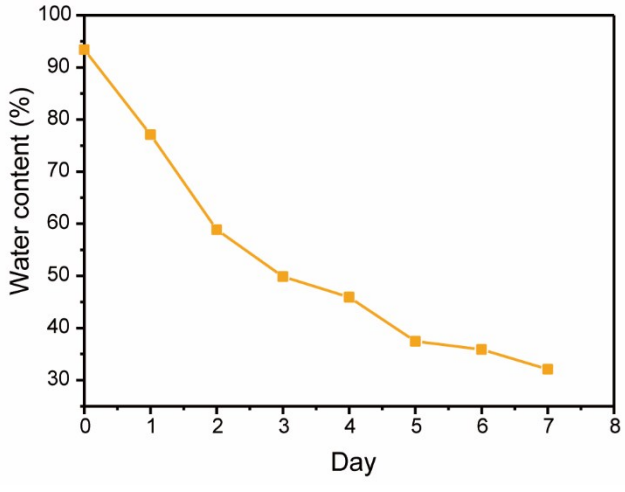

Figure S11. The water content change of $Ag/Ti_3C_2T_x$ hydrogel in 7 days in the air.

References

1. W. Qian, C. Yan, D. He, X. Yu, L. Yuan, M. Liu, G. Luo and J. Deng, *Acta Biomater.*, 2018, 69, 256-264.
2. M. C. Wu, A. R. Deokar, J. H. Liao, P. Y. Shih and Y. C. Ling, *ACS Nano*, 2013, **7**, 1281-1290.
3. B. Z. Ristic, M. M. Milenkovic, I. R. Dakic, B. M. Todorovic-Markovic, M. S. Milosavljevic, M. D. Budimir, V. G. Paunovic, M. D. Dramicanin, Z. M. Markovic and V. S. Trajkovic, *Biomaterials*, 2014, 35, 4428-4435.
4. W. Yin, J. Yu, F. Lv, L. Yan, L. R. Zheng, Z. Gu and Y. Zhao, *ACS Nano*, 2016, 10, 11000-11011.
5. W. Zhang, S. Shi, Y. Wang, S. Yu, W. Zhu, X. Zhang, D. Zhang, B. Yang, X. Wang and J. Wang, *Nanoscale*, 2016, 8, 11642-11648.
6. S. Wu, A. Li, X. Zhao, C. Zhang, B. Yu, N. Zhao and F. J. Xu, *ACS Appl. Mater. Interfaces*, 2019, 11, 17177-17183.
7. Q. Yin, L. Tan, Q. Lang, X. Ke, L. Bai, K. Guo, R. Qiao and S. Bai, *Appl. Catal. B-Environ.*, 2018, 224, 671-680.
8. W. N. Wang, P. Pei, Z. Y. Chu, B. J. Chen, H. S. Qian, Z. B. Zha, W. Zhou, T. Liu, M. Shao and H. Wang, *Chem. Eng. J.*, 2020, 397, 125488.
9. Y. Peng, Y. Liu, X. Lu, S. Wang, M. Chen, W. Huang, Z. Wu, G. Lu and L. Nie, *J. Mater. Chem. B*, 2018, 6, 2813-2820.
10. X. Xu, X. Liu, L. Tan, Z. Cui, X. Yang, S. Zhu, Z. Li, X. Yuan, Y. Zheng, K. W. K. Yeung, P. K. Chu and S. Wu,

Acta Biomater., 2018, 77, 352-364.

11. S. Tan, X. Wu, Y. Xing, S. Lilak, M. Wu and J. X. Zhao, *Colloid Surf. B-Biointerfaces*, 2020, 185, 110616.